Hyperbaric oxygen induces endogenous neural stem cells to proliferate and differentiate in hypoxic-ischemic brain damage in neonatal rats.

Submitted: 6/5/07 - Accepted: 10/11/07

Y-J YANG, X-L WANG, X-H YU, X. WANG, M. XIE, C-T LIU

Division of Neonatology, Department of Pediatrics, Xiang Ya Hospital, Central South University

Yang Y-J, Wang X-L, Yu X-H, Wang X, Xie M, Liu C-T. Hyperbaric oxygen induces endogenous neural stem cells to proliferate and differentiate in hypoxic-ischemic brain damage in neonatal rats. Undersea Hyperb Med 2008; 35(2):113-129. Background and purpose - Studies suggest that after brain injury, hyperbaric oxygen (HBO_2) is neuroprotective by stimulating cell proliferation. We examine whether HBO_2 promotes neural stem cells (NSC) to proliferate and differentiate in neonatal hypoxic-ischemic (HI) rats. Methods - Seven-day-old rat pups were subjected to unilateral carotid artery ligation followed by 2 hours of hypoxia (8% O_2). HBO_2 was administered (2 ATA (atmospheres absolutes), once daily for 7 days) within 3 hours after HI. The proliferating neural stem cells in the subventricular zone (SVZ) and dentate gyrus (DG) were dynamically examined by 5-bromo-2-deoxyuridine (BrdU)/nestin immunofluorescence. Nestin protein was detected by western blot analysis at various time points (from 6 hours to 14 days) after HI. The migrating NSC were examined by BrdU/doublecortin (DCX) immunofluorescence 7 and 14 days after HI. The phenotype of the newborn cells was identified by BrdU/β-tubulin, BrdU/ glial fibrillary acidic protein (GFAP) and BrdU/O_4 (oligodendrocyte marker) immunofluorescence. Myelin basic protein (MBP) was examined by immunohistochemistry and pathological changes of the brain tissue were detected 28 days after HI. Results – In neonatal HI rats treated with HBO_2, the proliferation of endogenous NSC was observed in the SVZ and DG. Cell numbers peaked 7 days after HI and proliferating NSC migrated to the cerebral cortex at 14 d after HI. Twenty-eight days after HI, an increase in newly generated neurons, oligodendrocytes and MBP was observed in the HBO_2 group compared to the untreated and HI-treated rats. Conclusions - This study suggests that HBO_2 treatment may promote neurogenesis of the endogenous NSC in neonatal HI rats, contributing to repair of the injured brain.

INTRODUCTION

Hypoxic-ischemic cephalopathy (HIE) is a common but severe complication of asphyxia that occurs during the perinatal period with a high rate of morbidity and mortality (1, 2). HIE is also the major recognized perinatal cause of neurological morbidity in full-term newborns (3) and can result in mental impairment, seizures and permanent motor deficits, such as cerebral palsy (4). At present, there are no effective means of repairing the hypoxic-ischemic brain damage (HIBD) once damage has occurred. Therefore, it is necessary that a suitable therapy for HIBD be developed.

Increasing knowledge of the renewal of cells within the central nervous system (CNS) has shed new light on severe HIBD. Furthermore, the discovery of neural stem cells (NSC) in mammals and the potential of these cells to regenerate lost areas of the CNS have allowed the development of new approaches to HIBD therapy. It has been reported that

endogenous NSC generally remain dormant. However, NSC may be activated in response to some diseases, for example cerebral ischemia, or by certain stimuli such as cell factors and growth factors (5). It has also been shown that proliferating NSC stimulated by brain damage are able to migrate to the affected areas and repair the brain damage (6). Since, such an approach would avoid the complex ethical and biological issues involved with embryonic stem cells or immortalized cell lines, the potential to recruit endogenous NSC to affected areas should be exploited in the development of new therapies. However, the capacity for recruiting endogenous NSC is limited (7,8). Thus, other strategies used to modify endogenous neurogenesis after ischemic brain injury have been described (9). Hyperbaric oxygen (HBO_2) therapy has been used in neonatal disease for many years (10). Due to concerns regarding the toxicity of oxygen, such as retinopathy of prematurity (11,12) and misunderstanding of HBO_2 therapy, the safety and validity of HBO_2 therapy has become questionable. However, HBO_2 therapy is quite different from oxygen treatment and no side effects have been found in HIBD neonatal rats after HBO_2 therapy to date (13-15). Furthermore, HBO_2 therapy was neuroprotective in hypoxic ischemic rat models (14-16). Thus, interest in HBO_2 therapy for hypoxic ischemic brain damage (HIBD) has increased.

In the past, mechanistic studies have focused mainly on reducing neuronal apoptosis and protecting the neurons, by for example stimulating the expression of endogenous basic fibroblast growth factor (bFGF) and alleviating the downstream activation of neurotrophin-3 (NT-3) in neonatal rats after hypoxia-ischemia (HI) (17-19). A recent study has shown that HBO_2 is neuroprotective by promoting cell proliferation in the brain (20). We have also found that HBO_2 therapy can protect the NSC and stimulate cell proliferation in the hippocampal dentate gyrus (DG) areas and subventricular zone (SVZ). These observations have prompted us to ask the following questions: i) are the cells that are stimulated to proliferate by HBO_2 NSC? Since the proliferating cells include astrocytes and NSC in the brain, BrdU/nestin immunofluorescence were used to double-label the proliferating NSC; ii) are the proliferating NSC stimulated by HBO_2 capable of migrating to the affected areas and differentiating into mature neurons? iii) is the neuroprotective effect induced by HBO_2 therapy associated with the proliferation of NSC? If this is the case, perhaps activation of endogenous NSC (that reside in the brain throughout life) could be induced by the application of HBO_2 in HIBD rats. Thus, in this study, we examined the proliferation of endogenous NSC, migration of neural progenitors and their long-term differentiation into neurons in neonatal HI rats.

MATERIALS AND METHODS

Animals

One hundred and eighty 7-day-old Sprague-Dawley rats of both genders (purchased from the Animal Department, Xiang Ya School of Medicine, Central South University, China), weighing 12.8-15.6 g, were randomly divided into 3 groups: 1) a normal control group (CON), 2) a HIBD group, and 3) a HBO_2 group in which HI rats were treated with HBO_2 (n=60 rats in each group). Each group was divided into 6 subgroups according to the time after HI as follows: HI-6 h, HI-24 h, HI-3 d, HI-7 d, HI-14 d and HI-28 d (n=10 rats in each group).

Animal model of HIBD

The protocol was evaluated and approved by the Animal Department of the XiangYa School of Medicine (Central South University, China). Seven-day-old Sprague-Dawley rats

were subjected to the Rice-Vannucci procedure (21), as described previously. Briefly, rats were anesthetized with ether, and the left carotid artery was sectioned permanently between double ligatures with 7-0 sterile surgical silk. The rats were allowed to recover for 1 ~ 2 hours, and then exposed to 2 hours of hypoxia in a plastic container that was perfused with a mixture of humidified 8% oxygen balanced with nitrogen. The temperature inside the container was maintained at 33°C, the temperature at which rat pups huddle with their mother. The pups were then returned to their mothers.

Hyperbaric oxygen exposure

The HBO_2 groups were administered HBO_2 treatment within 3 hours after HIBD. The HBO_2 treatment was administered for 60 minutes in a baby HBO_2 chamber (YLC0.5/1A, Wuhan, China) pressured with 100% oxygen to 2.0 atmospheres absolute (ATA). The oxygen concentration inside the cabinet was measured at the air vent by a mobile digital oxygen monitor (CY-12C, Hangzhou, China). A constant oxygen flow was given to maintain the oxygen concentration in the chamber at 85% or greater. Hyperbaric oxygen exposure was given once daily for 7 consecutive days. Carbon dioxide can be absorbed by natrica calx in the cabinet.

5-Bromo-2'-deoxyuridine labeling

Twenty-four hours after HIBD, animals were administered with 5-bromo-2'-deoxyuridine (BrdU; Sigma, St. Louis, MO, USA) intraperitoneally twice daily for 6 days (50 mg/kg, dissolved in saline).

Tissue preparation for microscopy

Animals were deeply anesthetized with chloral hydrate (450 mg/kg, intraperitoneally) at 6 sequential time intervals after HI (6 h, 24 h, 3 d, 7 d, 14 d, 28 d after HI; n = 10/sub-group) and underwent a transcardiac perfusion with 50-100 ml 0.9% saline, followed by 50-100 ml cold 4% paraformaldehyde in 0.1 M PBS (pH 7.4). The bregma was labeled with methylene blue and the brain was removed and post-fixed in paraformaldehyde for 24 hours. Tissue taken from 1.0 to -0.8 mm and - 3.0~ -4.5 anterior to the bregma, was processed, embedded in paraffin wax, and cut into 5 μm sections coronally (SM2000R, Leica, Nussloch, Germany) on polylysine–coated slides.

Hematoxylin-Eosine (HE) staining and Nissl staining

After de-waxing, the slides were stained with Hematoxylin-Eosine (HE) or Nissl-stained with toluidine blue for neuronal cell bodies. The brain sections were then mounted, air-dried, dehydrated, and coverslips were applied. Then the number of neurons in the cortex and hippocampal CA1 region was quantified according to the Nissl staining results. Cell morphology was examined by HE staining and Nissl staining.

Immunohistochemistry

Sections were de-waxed and the antigen was restored by microwaving. Sections were then blocked in 5 % bovine serum albumin (BSA, Sigma, USA) for 1 hour at 37°C. Sections were subsequently incubated with the primary antibodies at 4°C overnight. The specific primary antibodies used to identify the proliferating NSC were mouse anti-Nestin (1:200, Chemicon, Temecula, CA, USA) and rat anti-BrdU (1:200, Accurate Chemicals, Westbury, NY, USA). Rabbit anti-DCX (1:100, Cell Technology Signaling, Boston, USA), rabbit anti-β-tubulin (1:50, Cell Signaling Technology, Boston, USA), rabbit anti-Glial fibrillary acidic protein (GFAP) (1:100, Beijing Zhongshan Golden Bridge Biotechnology Co., Beijing, China), mouse anti-O4 (oligodendrocyte marker) (1:100, Chemicon) and rat anti-BrdU were used to identify the

newly generated cells. For BrdU processing, sections were incubated in 2 M HCl for 30 minutes at 37°C followed by 0.04% pepsin for 6 minutes at room temperature. Sections were incubated for 1 hour at 37°C in the dark with the following secondary antibodies: FITC-conjugated goat anti-mouse (1:100, Beijing Zhongshan Golden Bridge Biotechnology Co.) for Nestin or O4; FITC-conjugated goat anti-rabbit (1:100, Beijing Zhongshan Golden Bridge Biotechnology Co.) for GFAP, β-tubulin or DCX; and TRITC-conjugated goat anti-rat (1:100, Beijing Zhongshan Golden Bridge Biotechnology Co.) for BrdU. Sections were rinsed, and coverslips were placed. Immunoreactivity was observed using laser scanning confocal microscopy (LSM Invert 510; Zeiss, Jena, Germany).

For myelin basic protein (MBP) immunohistochemistry, rabbit anti-MBP was used. After blocking (0.3% H_2O_2 in PBS for 10 minutes at 4°C), specimens were incubated with rabbit anti-MBP primary antibody (1:100, Beijing Zhongshan Golden Bridge Biotechnology Co.) at 4°C overnight. After rinsing, sections were incubated with the biotin-conjugated anti-rabbit secondary antibody for 30 minutes at 37°C. Sections were treated with 3,3′-diaminobenzidine (DAB), rinsed, and coverslips were applied. MBP-positive cells were identified by light microscopy as brown-colored cells.

Western blot analysis

Animals were deeply anesthetized with chloral hydrate (450 mg/kg, intraperitoneally) at 5 sequential time intervals after HI (6 h, 24 h, 3 d, 7 d, 14 d after HI) and fresh tissue samples (approximately 100 mg) from the lesioned brain (bregma between 1.0 and – 4.5 mm) were obtained and placed on ice. Samples were then ground into fine powder and homogenized in a tissue-lysis buffer (0.1 mol/L NaCl, 0.01 mol/L Tris-HCl, 0.001 mol/L EDTA and 1 μg/ml aprotinin). Sodium dodecyl sulfate-polyacrylamide gel (SDS-PAGE, 5%) was performed under non-reducing conditions. Lysates from the brain tissue samples of every group were run on each gel, together with pre-stained low-molecular-weight markers (BioRad, Richmond, CA, USA). The proteins on the gel were subsequently transferred to the Immobillon PVDF transfer membrane (Bio lab, USA) in buffer containing 20% methanol, 39 mmol/L glycine, 48 mmol/L Tris base, and 0.4% SDS (pH 8.3). The membrane was blocked in 5% powdered milk in 0.01 M PBS for 1 hour. The membrane was then incubated for 2 hours with a mouse monoclonal antibody to Nestin (1:1000; Chemicon) at 4°C overnight. The membrane was washed with 0.1% TBS-Tween and then incubated with horseradish peroxide–conjugated anti-mouse IgG secondary antibody (1:10000, BioRad, USA) for 1 hour. After thorough washing, the positive band was revealed by ECL Western blotting detection reagents (KPL, Maryland, USA) and autoradiography film. Glyceraldehyde 3 phosphate dehydrogenase (GAPDH, Kangchen Biology, Shanghai, China)), an enzyme involved in glycolysis, was employed as a reference protein for the densitometric analyses.

Cell counting and semiquantitative protein estimation on blots

Quantification of $BrdU^+nestin^+$ (6 hours, 24 hours, 3 days, 7 days, 14 days after HI), $BrdU^+DCX^+$ (7 days, 14 days after HI), $BrdU^+$ β-$tubulin^+$ (28 days after HI) in cells from the SVZ and DG of the hippocampus and cerebral cortex at different time points were carried out using laser scanning microscope (LSM 510, Zeiss) by an investigator blind to the experimental groups. The relative amounts of Nestin protein were estimated directly from X-ray film by imaging densitometry (TANON 2020, Shanghai, China). In each case, results were obtained by calculating a ratio of nestin

protein to GAPDH protein levels and reported as relative optical density.

Statistical analysis

Data were expressed as mean ± standard deviation (SD). The differences between groups were examined for statistical significance using one-way ANOVA. MBP scores were analyzed using the Mann-Whitney U test. *P* value less than 0.05 was considered to be statistically significant.

RESULTS

Editorial note: due to the number and nature of the 11 graphics cited in the following pages, they have been placed, together, after the Acknowledgment section of this paper.

The proliferation of endogenous NSC in SVZ at different time points after HIBD

Cells positive for BrdU and nestin ($BrdU^+$ $nestin^+$) were considered to be proliferating NSC. As shown in Fig 1, $BrdU^+nestin^+$ cells were observed in the dorsal angulus lateralis of the SVZ in each group with proliferating cells migrating outwards. HBO_2 treatment significantly increased the number of $BrdU^+nestin^+$ cells in SVZ 6 hours after HI ($P<0.05$). Thereafter, the $BrdU^+nestin^+$ cells increased more gradually at 3 days ($P<0.01$) and peaked 7 days after HI ($P<0.05$). The number of $BrdU^+nestin^+$ cells decreased gradually 14 days after HI. Even so, more cells were observed in the HBO_2 group than in the CON and HIBD group ($P<0.05$, Fig. 1; Fig. 2).

In the blank controls (i.e. without injection of BrdU), no positive cells were observed in the SVZ.

The proliferation of endogenous NSC in DG at different time points after HIBD

Nestin protein is the most commonly used marker of NSC (22). This BrdU/nestin double staining was used to identify the proliferating NSC. As shown in Fig. 3, $BrdU^+nestin^+$ cells were observed in the hippocampal DG areas, predominantly distributed at the polymorphous cell layer and pyramidal layer. There was no significant difference between each group 6 hours after HI. HBO_2 treatment significantly increased the number of $BrdU^+nestin^+$ cells 24 hours after HI compared to the CON group ($P<0.05$). This increase occurred later than that observed in the SVZ. In the HBO_2 group, the number of $BrdU^+nestin^+$ cells peaked 7 days after HI ($P<0.01$) with $BrdU^+nestin^+$ cells number beginning to decrease 14 days after HI ($P<0.05$). However, at 14 days, a higher number of $BrdU^+nestin^+$ cells was still observed in the HBO_2 group compared to the CON and HIBD groups ($P<0.05$, Fig. 3, Fig. 4). In the blank controls (i.e. without injection of BrdU), no positive cells were observed in the DG.

Western blot analysis of Nestin protein at different time points after HI

The total protein in the lesioned cerebral hemisphere was examined by western blot analysis. Fig. 5 shows the effects of HBO_2 therapy on nestin protein levels at different time points after HIBD. An increase in nestin protein occurred in the HBO_2 group 24 hours after HI. Nestin levels peaked 7 days after HI. The nestin protein in the HBO_2 group was higher than that in the CON and the HIBD groups 3 days and 7 days after HI ($P<0.05$, Fig. 5).

Migration of NSC after HBO_2 treatment

DCX and BrdU were used in this study to identify newly generated neurons. Cells positive for BrdU and DCX ($BrdU^+DCX^+$) were observed in the SVZ in each group 7 days after HIBD, predominantly localized to the dorsal angulus lateralis (Figs.6-1; 6-2; 6-3). The $BrdU^+DCX^+$ cells were close-up in

the SVZ and a significantly higher number of $BrdU^+DCX^+$ cells were observed in the HBO_2 group compared with the CON and HIBD groups ($P<0.05$) (Fig. 6-4). The $BrdU^+DCX^+$ cells migrated along the gastral corpus callosum in a chain-like formation. Fewer $BrdU^+DCX^+$ cells were observed in other encephalic regions. The $BrdU^+DCX^+$ cells in the SVZ began to decrease 14 days after HIBD in the HBO_2 group (Fig.6-4). Simultaneously, more $BrdU^+DCX^+$ cells were observed in the cerebral cortex of the affected brain (Fig. 6-5). More $BrdU^+DCX^+$ cells were observed in the HBO_2 group with a higher percentage of neurons (71.4%±12.7%) compared with the CON and HIBD groups ($P<0.01$, Fig. 6-5). The number of $BrdU^+DCX^+$ cells in the cerebral cortex began to decrease 28 days after HIBD.

Differentiation of NSC into mature neurons, astrocytes and oligodendrocytes after HBO_2 treatment

The differentiation of NSC was monitored using β-tubulin, GFAP and O4 as markers for mature neurons, astrocytes and oligodendrocytes, respectively. As shown in Fig. 7, more $BrdU^+$β-$tubulin^+$ cells were observed in the affected cerebral cortex 28 days after HI in the HBO_2 group than in the CON group. The percentage of mature neurons (74.5±6.5%) was higher in the HBO_2 group compared with the CON and HIBD groups ($P<0.05$, Fig. 7). In comparison with the CON and HIBD groups, fewer astrocytes (i.e. $BrdU^+GFAP^+$ (16.8±5.8%)) and more oligodendrocytes (i.e. $BrdU^+O4^+$ (8.7±3.5%)) were observed in the cerebral cortex of the HBO_2 group ($P<0.05$, Fig. 7; Fig. 8).

HIBD reduced the MBP staining, while HBO_2 increased the MBP staining

Myelin Basic Protein (MBP) is a major constituent of the myelin sheath (23). MBP positive staining was clearly observed in the normal control rat brain, at the corpus callosum and striatum corpora of P35 rats. A grade system was used to score the intensity of MBP positive staining. The score was defined as follows: mild, 1; moderate, 2; strong, 3; and no immunoreactivity, 0. Digital microscopic images were taken at the corpus callosum and striatum corpora for each brain section. The average of the three scores was used to represent the grade of MBP staining for each brain. The MBP staining grade in the CON, HIBD and HBO_2 group rat brains was 2.0 ± 0.4, 0.8 ± 0.2, and 1.7 ± 0.3, respectively. Thus, HIBD significantly suppressed expression of MBP (Fig. 9.), whereas expression of MBP in the HBO_2 group rat brain was less affected. The MBP staining score in the HBO_2 group rat brain was significantly higher than that observed in the HIBD rat brain ($P<0.05$).

The enhanced recovery of neurons after HBO_2 treatment

HIBD in newborn rats results in diffuse damage. The long-term changes in CON, HIBD and HBO_2 rats were observed 28 days after HIBD (Fig. 10). HE staining in the CON group revealed that the neurons were organized correctly in the cortex (Fig.10). After HIBD, the cells in the cortex were disorganized. In particular, the cells had shrunk, the number of gliacytes had increased and a severe loss in the number of neurons was observed. However, after HBO_2 treatment, the pyramidal cells were organized, the nucleoli were clear, and fewer neurons were lost.

We also used Nissl staining with Toluidine blue to examine the tigroid body staining in neurons. Using light microscopy, the tigroid body stains dark blue and the cell nucleus stains blue. In the CON group, the neurons had normal morphology. More tigroid bodies were observed in the CON group than

in the HIBD and HBO_2 groups. However, more neurons and tigroid bodies were observed in the HBO_2 group than in the HIBD group ($P<0.01$). In the HBO_2 group, the nuclei and nucleoli were clearly observed **(**Fig.10-2; Fig. 10-3; Fig.11).

DISCUSSION

Apoptosis or necrosis occurring in the neurons in the brain after perinatal HI insults might contribute to the delayed brain atrophy. Since, the hippocampus and the cortex are susceptible to HI injury (13), we analyzed these regions of the brain. The pathomorphology data obtained from this study shows dramatic neuronal loss in the cerebral cortex and hippocampal CA1 in HIBD rats compared with the CON group, indicating that it is impossible for the brain to repair the damage itself. We hypothesized that if the renewal capability of the endogenous NSC could be increased then the brain may be able to repair some of the damage. Here, we examine whether HBO_2 treatment promotes NSC proliferation and differentiation in neonatal HI rats. We show that after HBO_2 treatment, the number of neurons in the cerebral cortex and CA1 regions increased compared with the HIBD group, indicating that HBO_2 therapy contributes to self-recovery and protection of the affected brain. HBO_2 treated animals were also observed functional improvement. High oxygen may cause bronchopulmonary dysplasia (BPD) or retinopathy of prematurity (ROP) in neonatal animals, but HBO_2 therapy at the pressure under 3 ATA will not cause BPD or ROP (24). Therefore, our experiment was designed to apply the HBO_2 therapy once daily for consecutive 7 times at the pressure of 2.0 ATA according to our clinical experience.

Proliferating cells were labeled with BrdU. Thus, we assumed that $BrdU^+$ cells were proliferating cells [24]. In the developing brain, proliferating cells include NSC and astrocytes, so an increase in $BrdU^+$ cells does not reflect proliferation of NSC alone. Nestin, an intermediate filament protein, expressed in NSC as well as in lineage-constricted progenitors, immature neurons and some gliacytes, is widely used to identify, isolate or purify NSC. Thus, in this study, we used BrdU and Nestin double staining to distinguish between proliferating NSC and astrocytes.

In the mammalian brain, neurogenesis persists mainly in two germinal areas, the SVZ along the lateral wall of the lateral ventricles and the hippocampal DG (25). Newly generated neural precursors are recruited from the SVZ to nearby infracted areas (26,27). Some precursors express region-appropriate phenotypes, where continuous postnatal neuronal production seems to be supported by NSC. We show that HBO_2 therapy significantly increased the number of $BrdU^+nestin^+$ cells compared to that observed in the CON group, suggesting that HBO_2 therapy can promote the proliferation of endogenous NSC. Our study also showed that 7 days after HBO_2 therapy, the number of $BrdU^+nestin^+$ cells peaked. On-going studies in our laboratory are examining whether repeated treatments of HBO_2, administered after neonatal HIBD, contribute to enhancing this endogenous regenerative capacity. Western blot analysis revealed similar results: in the HBO_2 group, nestin protein levels began to increase 6 hours after HIBD, with levels peaking 7 days after HI. These observations indicate that HBO_2 treatment is neuroprotective to NSC and that this function is associated with the proliferation of NSC. Our study also found that more $BrdU^+nestin^+$ cells were observed in the SVZ. It has been argued that proliferating NSC originate mainly from the SVZ, and that the NSC observed in the DG have migrated from the SVZ (28).

Although HBO_2 treatment can promote the proliferation of NSC, it is essential to know

whether these NSC survive, differentiate into neurons and repair the injured brain. It has been shown that less migratory cells survive after brain damage (29). However, most cells die before differentiation, by a process that is known as selectivity survival and may be controlled by cytokines or signal transduction pathways in the niches (30,31), such as the Wnt/β-catenin pathway (32). Thus, in this study we examined whether HBO_2 improves the niches and promotes migration and differentiation of the NSC. We observed the dynamic migration and differentiation of NSC in the lesioned brain. One week after HI, more $BrdU^+DCX^+$ cells (newly generated immature neurons and migrating progenitors) were observed in the SVZ of the HBO_2 group than in the CON and HIBD groups, indicating that HBO_2 was capable of promoting the differentiation of NSC. The $BrdU^+DCX^+$ cells began to decrease 14 days after HI. $BrdU^+DCX^+$ cells were observed in the injured cerebral cortex with a higher neuronal percentage (71.4±12.7%), implying that HBO_2 treatment was conducive to the migration and differentiation of NSC into predominantly neurons. β-tubulin, GFAP and O4 were the mature marker of neurons, astrocytes (33) and oligodendrocytes (34) respectively. Twenty-eight days after HI, a decrease in $BrdU^+$ DCX^+ cells with an increase in $BrdU^+$β-$tubulin^+$ and $BrdU^+O_4^+$ cells was observed. Fewer $BrdU^+GFAP^+$ cells were observed in the injured brain, indicating that the newborn progenitors survived, and differentiated into mature neurons and oligodendrocytes. Whether these new cells are capable of replacing the injured brain tissue and forming a functional neural network still needs further examination. MBP, derived from oligodendrocytes, accounts for 40% of the whole myelin sheath protein and is the protein in the neuropile of the CNS. Unlike adult rats, newborn rats are more susceptible to white matter damage with a decrease in MBP occurring (35). In our study, more newly generated oligdendrocytes were observed in the HBO_2 group with less MBP lost, indicating that HBO_2 therapy promotes the NSC to differentiate into oligodendrocytes and recover the white matter damage.

In conclusion, our results indicate that HBO_2 treatment could promote the proliferation of endogenous NSC. We show that proliferating cells are capable of migrating to the injured brain and differentiating into mature neurons and oligodendrocytes in the neonatal HI brain, thereby repairing the brain damage. Whether the newborn neurons were capable of completely replacing the injured neurons, developing synaptic linkage and forming neural networks is currently being investigated in our laboratory.

ACKNOWLEDGMENTS

Projects supported by National Natural Science Foundation of China (the Science Fund of the Chinese Academy of Sciences), Grant 30672240.

We would like to thank Professor Feng-Jie Li and Dr. Yan-Song Zhao for their excellent technical assistance.

Figures 1 - 11

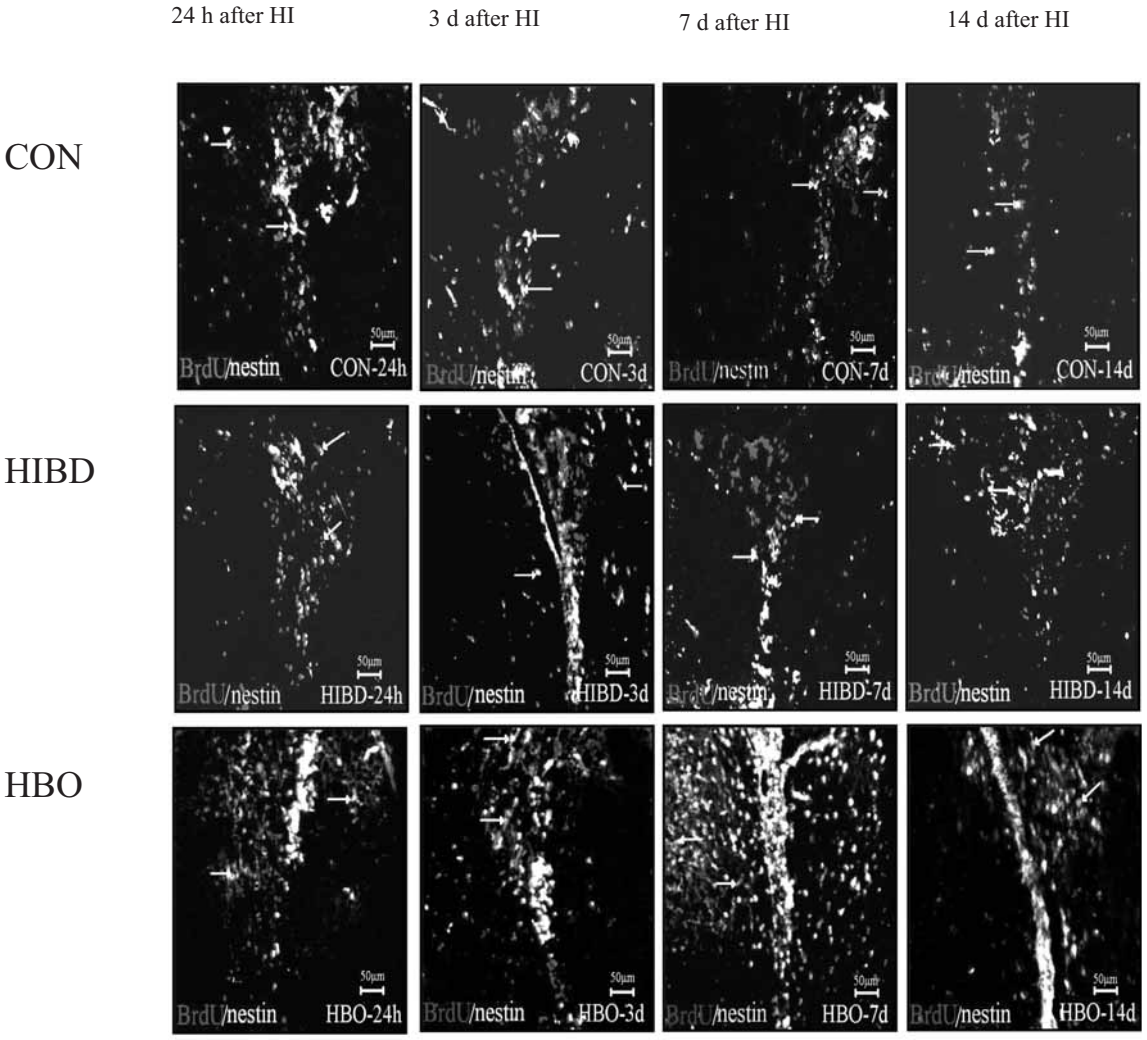

Fig.1. Effects of HBO therapy on endogenous NSC in the SVZ different time after HI. The proliferating NSC in the SVZ were examined at 24 h, 3 d, 7 d and 14 d after HI and the immunofluorescence staining was analyzed by confocal laser scanning microscope (LSM 510, Zeiss, Germany). The proliferating endogenous NSC were double labeled by BrdU/nestin, (the BrdU+ cells were stained in the nuclear and the nestin+ cells were stained in the cytoplasm, arrow). The top row is the CON group, the BrdU+ nestin+ cells decreased gradually after birth. The middle row is the HIBD group. The bottom row is the HBO group. In this Group, BrdU+ nestin+ cells remained a kind of proliferating status after HBO treatment till they reached the highest level 7 d after HI. The scale bar was labeled in each figure.
Abbreviations: BrdU, 5-bromo-2-deoxyuridine; NSC, neural stem cells; SVZ, subventricular zone; hypoxia ischemia, HI; HBO, hyperbaric oxygen; CON, the control group; HIBD, the hypoxic ischemic brain damage.

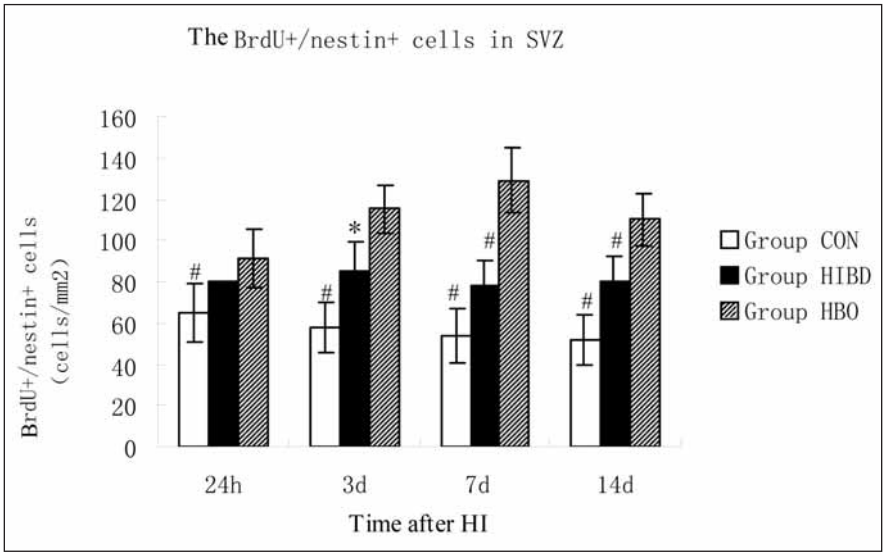

Fig.2 The bar chart of proliferation of NSC in the SVZ different time after HI Quantitative data of BrdU+ nestin+ cells in the SVZ different time after HI are shown in the bar chart. Note a remarkable increase in BrdU+ nestin+ cells especially at 7 d and 14 d after HI as compared with the HIBD group. Error bars show standard deviation, * indicates P<0.05 vs. the HBO group; # indicates P<0.01 vs. the HBO group.

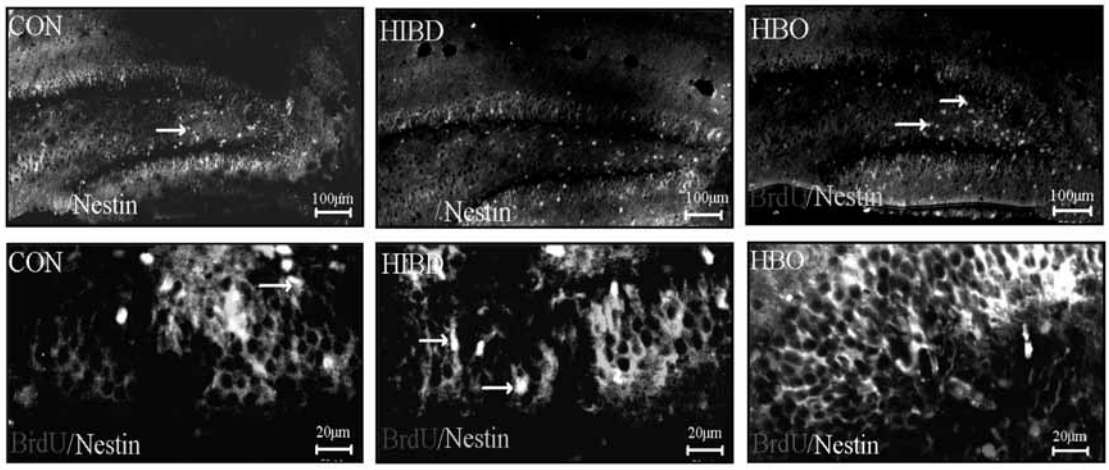

Fig. 3. Effects of HBO therapy on endogenous NSC in DG different time after HI. The proliferation of endogenous NSC in hippocampal DG 7 days after HI The proliferating NSC were double-labeled by BrdU/nestin (the BrdU+ cells were stained in the nuclear and the nestin+ cells were stained in the cytoplasm, arrow). The first row and second row are low and high magnification of BrdU+ nestin+ cells in DG respectively. The scale bar was labeled in each figure.
Abbreviations: BrdU, 5-bromo-2-deoxyuridine; NSC, neural stem cells; DG, dentate gyrus.

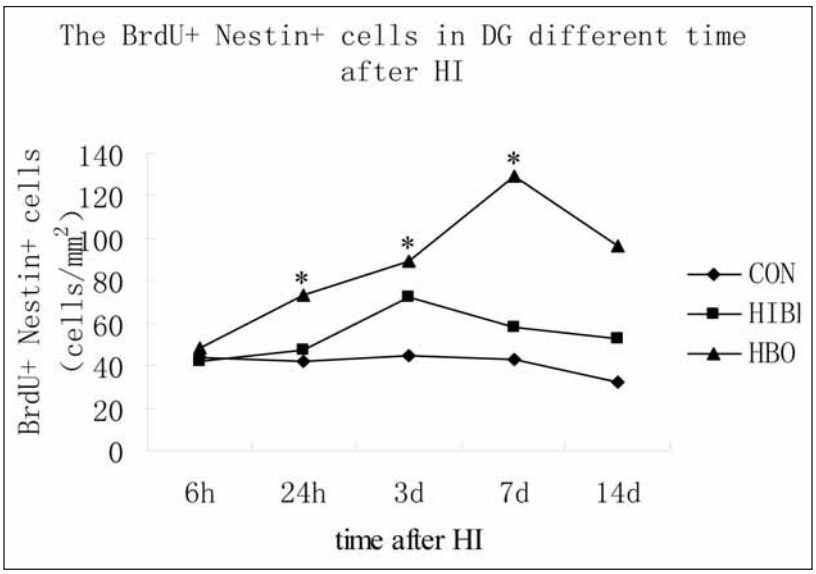

Fig.4. The dynamic changes of proliferating NSC different time after HI in DG The curve chart showed the changing tendency of proliferating NSC in every group and noted the significant difference. The proliferating NSC reached the highest level 7 d after HIBD. * indicates $P<0.05$ vs. the former time point.

Fig. 5-1

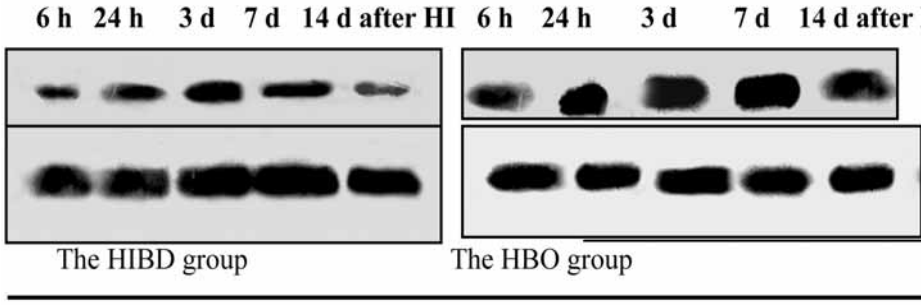

Fig. 5-1. Effects of HBO therapy on Nestin protein different time after HI. Western blots analysis of nestin protein. Western blots were performed on the left cortex of rats from Group CON, Group HIBD and Group HBO at 6 h, 24h, 3d, 7d, 14d after HI (n=10 per time point). The inset depicts representative western blots for nestin of each group at different time after HI. In each case, a representative band (170kD) is shown as well as a corresponding GAPDH (36kD). The band of nestin at 6 h, 24h, 3d, 7d, 14d after HI in both the HIBD group and the HBO group.

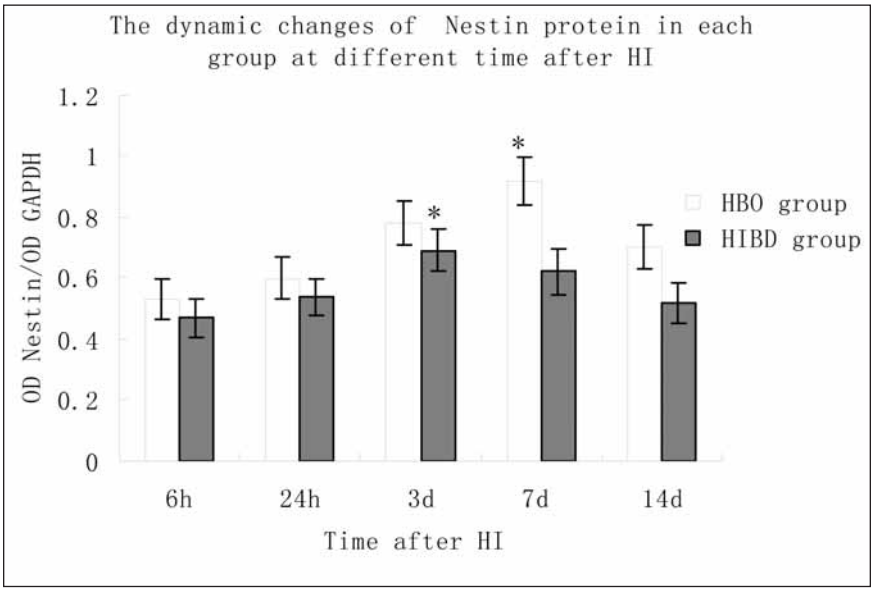

Fig. 5-2. Quantification of nestin protein in the left brain different time after HI The expression levels of the nestin protein was normalized to GAPDH protein by densitometric evaluation and presented as OD ratio. Error bars show standard deviation; * indicates P<0.05 significant higher as compared with all other subgroup in HIBD group or in the HBO group.

Fig. 6-1

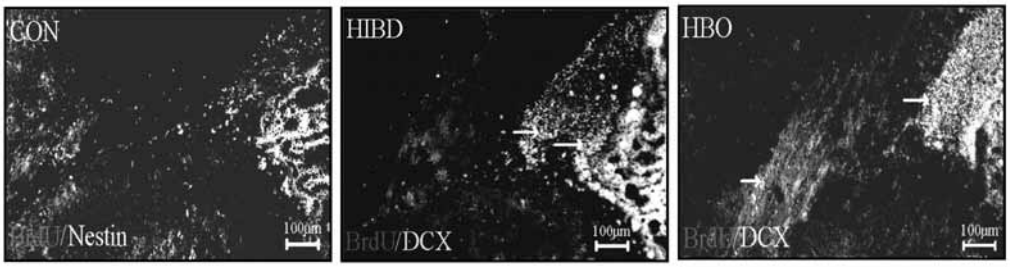

Fig. 6-2

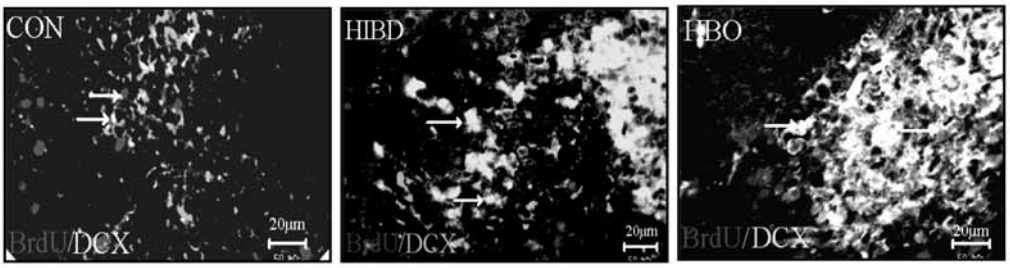

Fig. 6-3

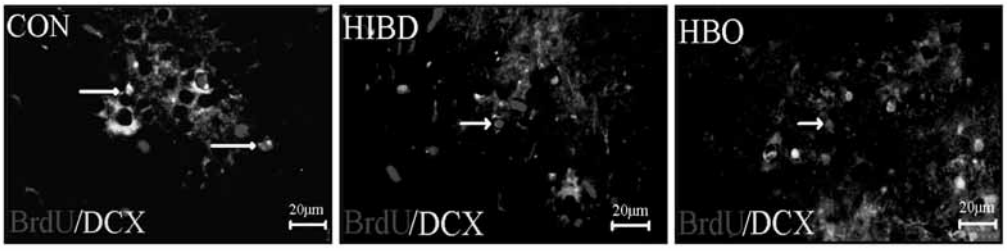

Fig. 6-4

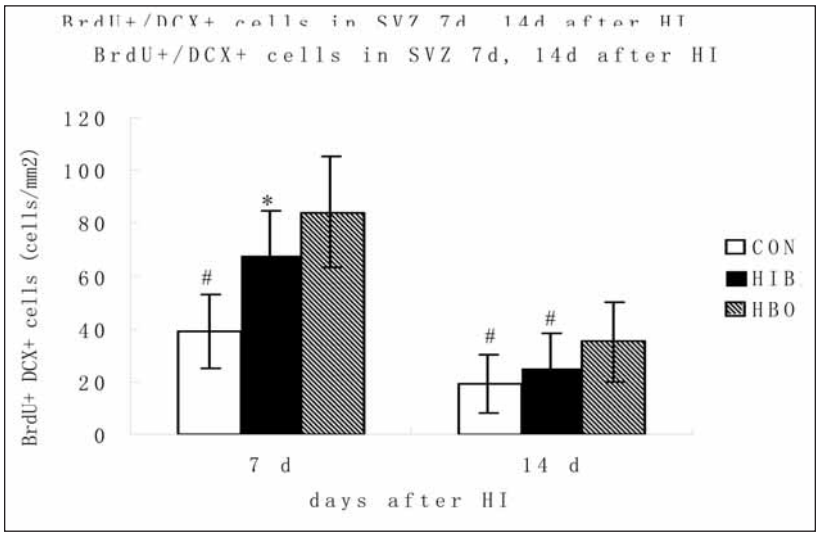

Fig. 6-5

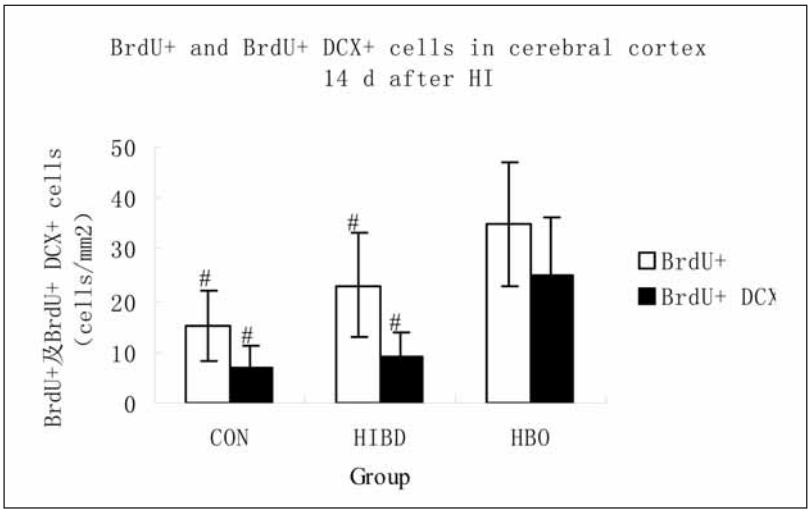

Fig.6 Migration and Differentiation of Endogenous Neural stem cells after HBO Therapy. **Fig.6-1, Fig.6-2.** Confocal image of BrdU/DCX double-labeled immunofluorecence 7 d after HI of a low and high magnification respectively. **Fig.6-3.** Confocal image of BrdU/DCX double-labeled imunofluorecence 14 d after HI. The migrating cells were doubly immunopositive for BrdU in the nucleus and DCX in the cytoplasm (arrow), more BrdU+ DCX+ cells were observed in the HBO group. The scale bar was labeled in each figure. **Fig.6-4.** Quantification of BrdU+ DCX+ cells in SVZ 7 d, 14 d after HI. Error bars show standard deviation; *indicates $P<0.05$ vs. Group HIBD; #indicates $P<0.01$ vs. the HBO group at different time points. **Fig.6-5** Quantification of BrdU+ and BrdU+ DCX+ cells in cerebral cortex 14 d after HI. Error bars show standard deviation; # indicates $P<0.01$ vs. the HBO group. Abbreviations: DCX, doublecortin.

Fig. 7-1

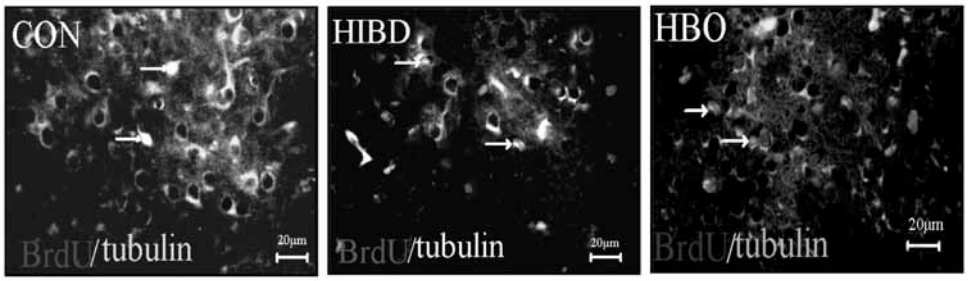

Fig. 7-2

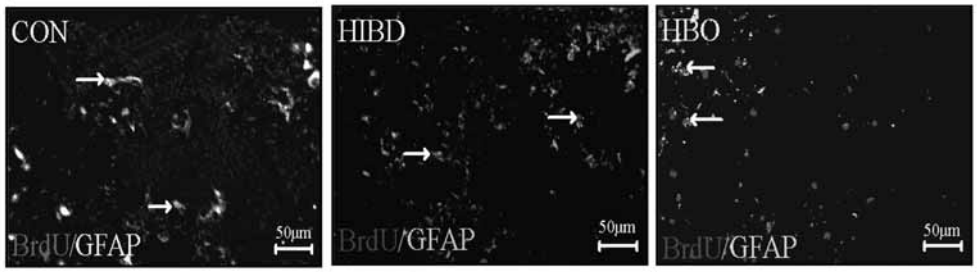

Fig. 7-3

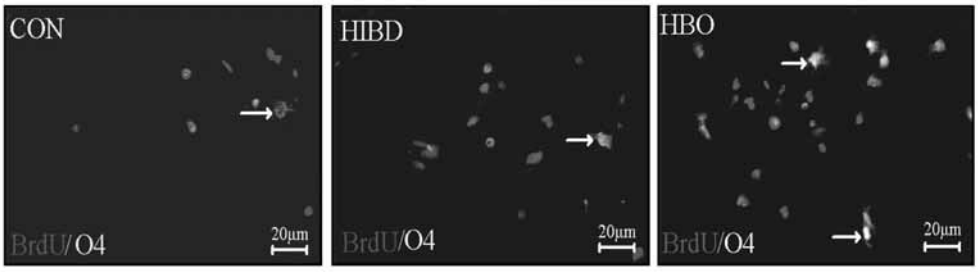

Fig.7. Differentiation of endogenous neural stem cells after HBO treatment **Fig.7-1**. BrdU/β-tubulin double staining of cerebral cortex The BrdU+ cells were stained in the nuclear and the β-tubulin+ cells were stained in the cytoplasm. Arrows in the figures indicate BrdU+ β-tubulin+ cells (newborn mature neurons). The scale bar was labeled in each figure. **Fig.7-2.** BrdU/GFAP double staining of cerebral cortex The BrdU+ cells were stained in the nuclear and the GFAP+ cells were stained in the cytoplasm. Arrows in the figures indicate BrdU+ GFAP+ cells (newborn mature astrocytes). **Fig.7-3.** BrdU/O4 double staining of cerebral cortex The BrdU+ cells were stained in the nuclear and the O4+ cells were stained in the cytoplasm. Arrows in the figures indicate BrdU+ O4+ cells (newborn oligodendrocytes). The scale bar was labeled in each figure.
Abbreviations: GFAP, glial fibrillary acidic protein; O4, oligodendrocyte marker.

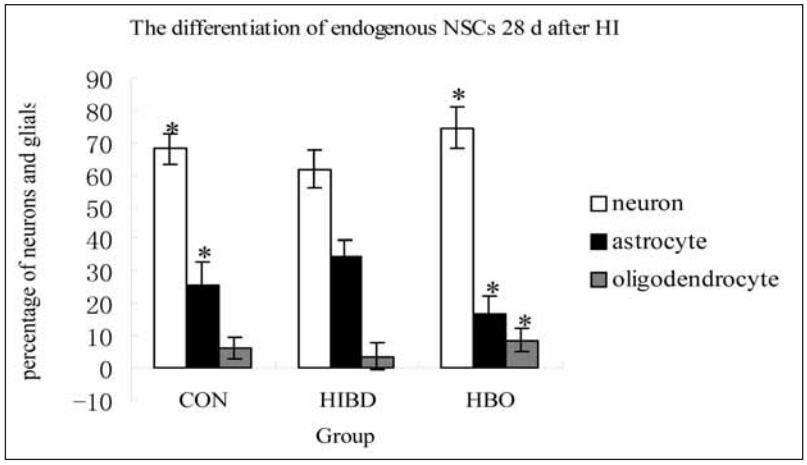

Fig.8. The differentiation of endogenous NSC 28 days after HI The bar chart showed the differentiation percentage of endogenous NSC to neurons, astrocytes and oligodendrocytes, that is the BrdU+ β-tubulin+, BrdU+ GFAP+, BrdU+ O4+ cells to BrdU+ cells. Error bars show standard deviation; * indicates $P<0.05$ vs. the HIBD group.

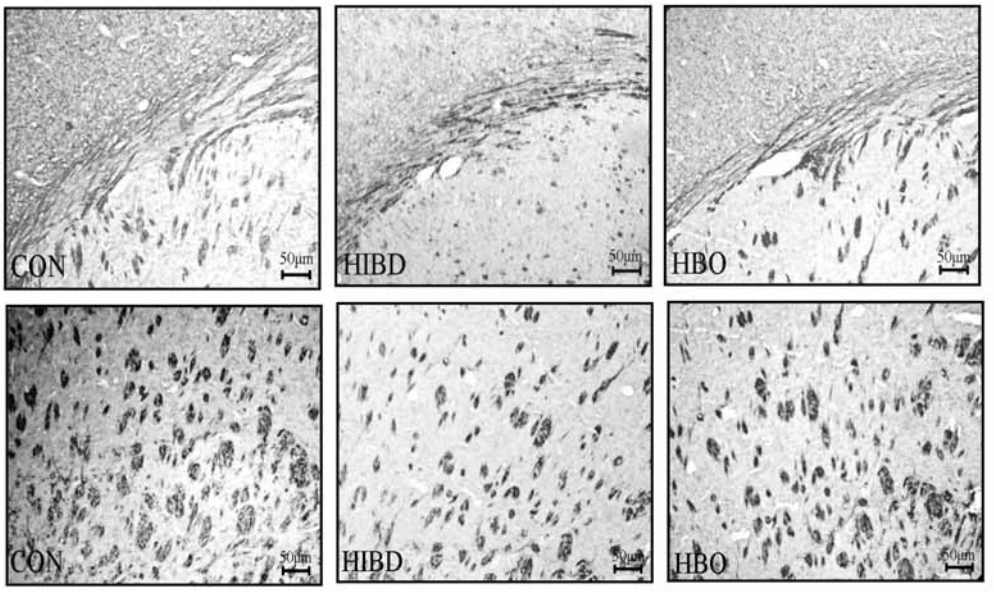

Fig. 9. Effects of HBO therapy on MBP protein. The MBP protein was immunostained in the brain section of 35-d-old rats. MBP positive staining (brown color) was observed at the corpus callosum area (the first row) and striatum corpora area (the second row). HIBD suppressed the expression of MBP. Expression of MBP in the rat brain treated with HBO was less affected. The scale bar was labeled in each figure. Abbreviations: MBP, myelin basic protein.

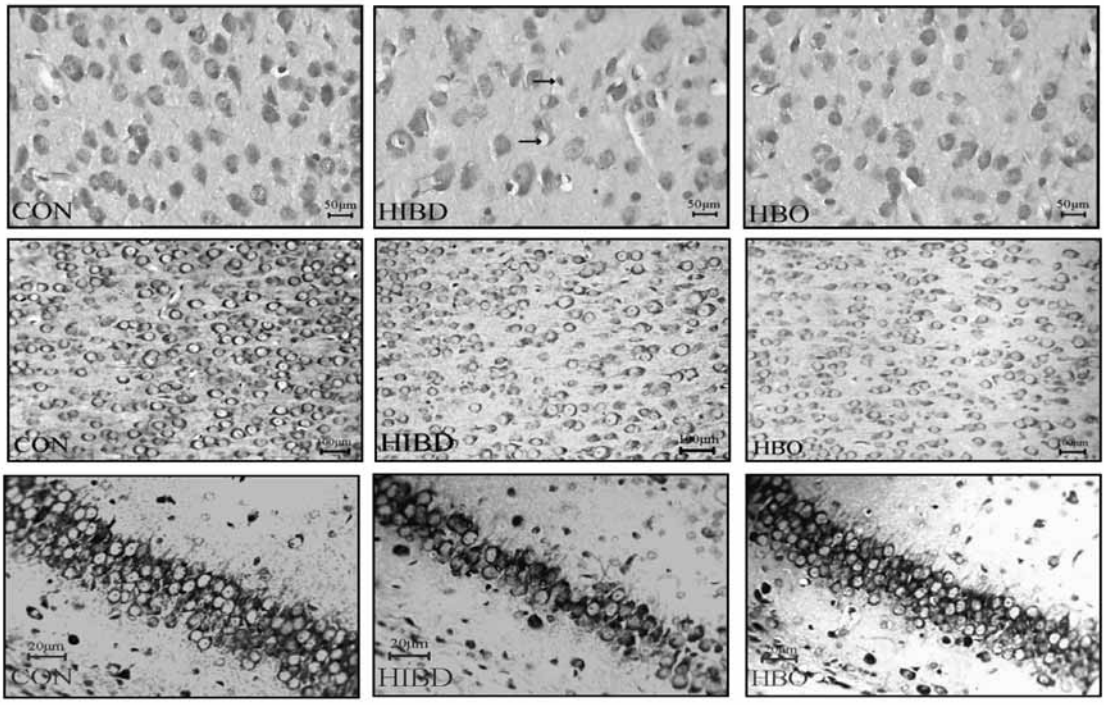

Fig.10. Degeneration of Neurons after HI and recovery of neurons after HBO treatment. The top row is the hematoxylin-eosine(HE)staining of cerebral cortex, arrows in the figure indicated cells with vacuolar degeneration or pycnotic nucleus; the middle row is nissl staining of cerebral cortex (including cells almost all layers); the bottom row is the nissl staining of hippocampal CA1 region, the tigroid body was stained dark, and the nucleole can be seen. The scale bar was labeled in each figure.

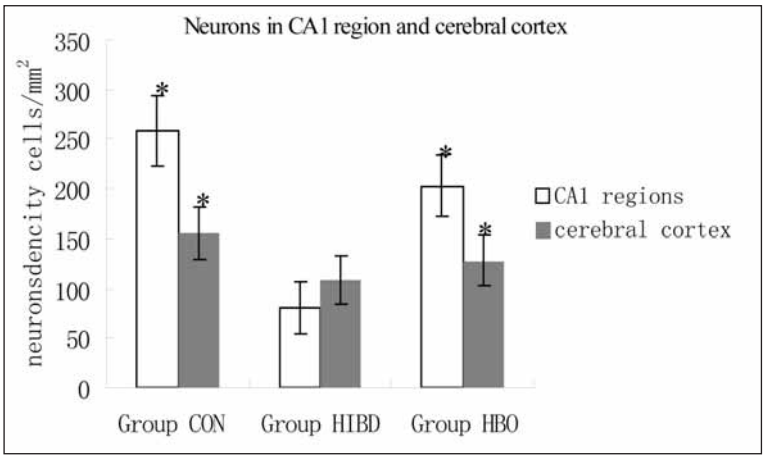

Fig.11. Quantification of the Loss and Recovery of Neurons in cerebral cortex. Changes in neuron numbers in cerebral cortex and CA1 pyramidal layers in CON, HIBD and HBO-treated animals (mean ± standard deviation obtained from10 animals) 28 d after HI. Error bars show standard deviation; * indicates P<0.01 vs. Group HIBD.

REFERENCES

1. Shah P, Riphagen S, Beyene J, Perlman M. Multiorgan dysfunction in infants with post-asphyxial hypoxic-ischemic encephalopathy. *Arch Dis Child Fetal Neonatal Ed* 2004; 89: 152-155.
2. Tsuji M, Wilson MA, Lange MS, Johnston M. Minocycline worsens hypoxic-ischemic brain injury in a neonatal mouse model. *Exp Neurol* 2004; 189: 58-65.
3. Triulzi F, Parazzini C, Righini A: Patterns of damage in the mature neonatal brain. *Pediatr Radiol* 2006; 36: 608 - 620.
4. Fawke J, McIntyre J. Recent advances in neonatology. *Curr Opin Obstet Gynecol* 2002; 14: 153-158.
5. Gage FH. Mammalian neural stem cells. *Science* 2000; 287: 1433-1438
6. Maslov AY, Barone TA, Plunker RJ, Pruitt SC., Neural stem cell detection, characterization and age-related changes in the subventricular zone of mice. *J Neurosci* 2004; 24: 1726-1733.
7. Parent JM, Vexler ZS, Gong C, Derugin N, Ferriero DM. Rat forebrain neurogenesis and striatal neuron replacement after focal stroke. *Ann Neurol* 2002; 52: 802-813.
8. Goings GE, Sahni V, Szele FG. Migration patterns of subventricular zone cells in adult mice change after cerebral cortex injury. *Brain Res* 2004; 996: 213-26.
9. Felling RJ, Snyder MJ, Romanko MJ, Rothstein RP, Ziegler AN, Yang Z, Givogri MI. Bongarzone ER, Levison SW. Neural stem/progenitor cells participate in the regenerative response to perinatal hypoxia/ischemia. *J Neurosci* 2006; 26: 4359-4369.
10. Rudge FW. Carbon monoxide poisoning in infants: treatment with hyperbaric oxygen. *S. Med. J* 1993; 86: 334–337.
11. Calvert J, Yin W., Patel M., Badr A., Mychaskiw G., Parent A., Zhang J. Hyperbaric oxygenation prevented brain injury induced by hypoxia–ischemia in a neonatal rat model, *Brain Res* 2002; 951: 1-8.
12. Badr AE, Yin W, Mychaskiw G, Zhang JH: Dual effect of HBO_2 on cerebral infarction in MCAO rats. *Am J Physiol Regul Integr Comp Physiol* 2001; 280: 766 - 770.
13. Calvert JW, Zhou C, Nanda A, Zhang JH, Effect of hyperbaric oxygen on apoptosis in neonatal hypoxia—ischemia rat model. *J Appl Physiol* 2003; 95: 2072~2080.
14. Vehkamp R.Siebing DA. Heiland S, Schoenffeldt-Varas P, Veltkamp C, Schwaninger M, Schwab S. Hyperbaric oxygen induces rapid protection against cerebral ischernia. *Brain Res* 2005; 1037: 134-138.
15. Günther A, Küppers-Tiedt L, Schneider PM, Kunert I, Berrouschot J, Schneider1 D, Roßner S. Reduced infarct volume and differential effects on glial cell activation after hyperbaric oxygen treatment in rat permanent focal cerebral ischaemia. *European Journal of Neuroscience* 2005; 21: 3189-3194.
16. Yang JY, Chang CN,Lee TH,Lin TN, Hsu JC, Hsu YH, Wu JH. Hyperbaric oxygen treatment decreases post-ischemic neurotrophin-3 mRNA down-

regulation in the rat hippocampus. *J Neuroreport* 2001; 12: 3589-3592.

17. Liberto PJ, Albrecht LM, Herx VW, Yong VW, Levison SW. Pro-regenerative properties of cytokine-activated astrocytes. *Journal of Neurochemistry* 2004; 89: 1092-1100.
18. Gutsaeva DR, Suliman HB, Carraway MS, Demchenko IT, Piantadosi CA. Oxygen-induced mitochondrial biogenesis in the rat hippocampus. *Neuroscience* 2006; 137: 493-504.
19. Rice JE, Vannucci RC, Brierley JB. The influence of immaturity on hypoxic-ischemic brain damage in the rat. *Ann Neurol* 1981; 9: 131-141.
20. Hermann A, Maisel M, Wegner F, Liebau S, Kim DW, Gerlach M, Schwarz J, Kim KS, Storch A. Multipotent neural stem cells from the adult tegmentum with dopaminergic potential develop essential properties of functional neurons. *Stem cells* 2006; 24: 949-964.
21. Iwai M, Ikeda T, Hayashi T, Sato K, Nagata T, Nagano I, Shoji M, Ikenoue T, Abe K. Temporal profile of neural stem cell proliferation in the subventricular zone after ischemia/hypoxia in the neonatal rat brain. *Neurol Res* 2006; 28: 461-468
22. Suzuki S, Gerhold LM, Bottner M, Rau SW, Dela Cruz C, Yang E, Zhu H, Yu J, Cashion AB, Kindy MS, Merchenthaler I, Gage FH, Wise PM. Estradiol enhances neurogenesis following ischemic stroke through estrogen receptors alpha and beta. *J Comp Neurol* 2007; 500: 1064-1075.
23. Cavre M, Bancila M, Virard I, Borges A, Durbec P. Migrating and myelinating potential of subventricular zone neural progenitor cells in white matter tracts of the adult rodent brain. *Mol Cell Neurosci* 2006; 31: 748-758.
24. Zhang JH, Lo T, Mychaskiw G, Colohan A. Mechanisms of hyperbaric oxygen and neuroprotection in stroke. *Pathophysiology* 2005; 12: 63-77.
25. Komitova M, Mattsson B, Johansson BB, Eriksson PS. Enriched environment increases neural stem/progenitor cell proliferation and neurogenesis in the subventricular zone of stroke-lesioned adult rats. *Stroke* 2004; 36: 1278-1282.
26. Yan YP, Sailor KA, Vemuganti R, Dempsev RI. Insulin-like growth factor-1 is an endogenous mediator of focal ischemia-induced neural progenitor proliferation. *Euro J Neurosci* 2006; 24: 45-54.
27. Romanko MJ, Rothstein RP, Levison SW. Neural stem cells in the subventricular zone are resilient to hypoxia/ischemia whereas progenitors are vulnerable. *J Cereb Blood Flow Metab* 2004; 24: 814-825.
28. Ourednik J, Ourednik V, Lynch WP. Neural stem cells display an inherent mechan ism for rescuing dysfunctional neurons. *Nat Biotechnol* 2002; 20: 1103-1110.
29. Nakatomi K, Yoshikawa M, Oka M, Ikegami Y, Hayasaka S, Sano K, Shiozawa K, Kawabata S, Soda H, Ishikawa T, Tanabe S, Kohno S. Transport of 7-ethyl-10-hydroxycamptothecin (SN-38) by breast cancer resistance protein ABCG2 in human lung cancer cells. *Biochem Biophys Res Commun* 2001; 288: 827-832.
30. Miller RH. The promise of stem cells for neural repair. *Brain Res* 2006; 1091: 258-264.
31. Imitola J, Raddassi K. Park KI, Mueller FJ, Nieto M, Teng YD, Frenkel D, Li J, Sidman RL, Walsh CA, Snyder EY, Khoury SJ. Directed migration of neural stem cells to sites of CNS injury by the stromal cell-derived factor1 alpha/CXC chemokine receptor 4 pathway. *Proc Natl Acad Sci* 2004; 101: 18117-18122.
32. Levison SW, Rothstein RP, Romanko MJ, Snyder MJ, Meyers RL, Vannucci SJ. Hypoxia/ischemia depletes the rat perinatal subventricular zone of oligodendrocyte progenitors and neural stem cells. *Dev Neurosci* 2001; 23: 234-247.
33. Hirabayshi Y, Gotoh Y. Stage-dependent fate determination of neural precursor cells in mouse forebrain. *Neuroscience Res* 2005; 51: 331-336.
34. Lendahl U, Zimmerman LB, Mckay RDG. CNS stem cells express a new class of intermediate filament p rotein. *Cell* 1990, 60: 585 -595.
35. Glaser T, Perez-Bouza A, Klein K, Brüstle O. Generation of purified oligodendrocyte progenitors from embryonic stem cells. *The FASEB Journal express* 2004, 10: 1-20.
36. Cai Z, Lin S, Pang Y, Rhodes PG. Brain Injury Induced by Intracerebral Injection of Interleukin-1beta and Tumor Necrosis Factor-alpha in the Neonatal Rat. *Pediatric Research* 2004; 56: 377-384.